Chinese Journal of Chemistry, **2009**, *27*, 1891—1896 **Full Paper**

Theoretical Investigation on Electronic Transition of Tris(8-quinolinolate) Aluminum Grafted on Poly(*p*-phenylenevinylene) Units with the Localized-density-matrix Method

SUN, Gang[a,b](孙刚) ZHANG, Min[a](张岷) YANG, Guochun[a](杨国春)
ZHAO, Liang[a](赵亮) FU, Qiang[a](傅强) SU, Zhongmin*,[a](苏忠民)

[a] *Institute of Functional Material Chemistry, Northeast Normal University, Changchun, Jilin 130024, China*
[b] *Chemistry and Biology Academy, Beihua University, Jilin, Jilin 132013, China*

An unsystematic molecule PPV-Alq_3 [3-(4-((*E*)-2-(8-hydroxy-3-(4-styrylstyryl)quinolin-Alq_2-6-yl)vinyl)-styryl)-6-(4-styrylstyryl)quinolin-8-olate-Alq_2; q = 8-quinolinolate], which combines poly(*p*-phenylenevinylene) with tris(8-quinolinolate)aluminum, has been studied using a localized-density-matrix method. The absorption spectra and electronic transition properties were analyzed and compared with both intermediate neglect of the differential overlap method and the localized-density-matrix method. Great efforts have been made on investigating conjugated system on the absorption properties as these can be particularly important for many applications. Two different absorptions of the special molecule, tris(8-quinolinolate)aluminum grafted on poly(*p*-phenylenevinylene) units, were further discussed with density matrices. For the molecule, the first absorption peak is at 413 nm near the purple light. Two 8-hydroxyquinolines have very slight electronic transition properties. Another absorption peak is at 237 nm. The second characteristic peak of molecule is completely different from that of the first one, which comes from contribution of 8-hyroxyquinolines in the two different side chains. Our studies show that electronic transition properties of poly(*p*-phenylenevinylene) can be effectively tuned by grafting tris(8-quinolinolate)-aluminum on poly(*p*-phenylenevinylene) from the standpoint of transition energies, frontier molecular orbitals and density matrices.

Keywords localized-density-matrix (LDM), intermediate neglect of the differential overlap (INDO), electronic transition, electron density

Introduction

Photoluminescence (PL) and electroluminescence (EL) have been extensively studied on small molecules and polymer materials due to their important applications. While tris(8-quinolinolate)aluminum (Alq_3) is known as the typical small molecule in organic light-emitting diodes (OLED), it has a variety of technical applications since the first realization of a multilayered EL was devised by Tang and Vanslyke in 1987.[1] Alq_3 and its two isomers, as the most common and important organic electroluminescence material in many experiments,[2-5] have been extensively studied. In addition, its theoretical investigations have been also discussed,[6-9] for example, some groups incorporated with the 8-hydroxyquinoline were inducted or Al was replaced by other metals.[10,11] On the other hand, π-conjugation organic polymers have been extensively studied as they play important roles in OLED since the discovery of poly(*p*-phenylenevinylene) (PPV) in 1990.[12] Therefore, PPV has been extensively studied due to its high fluorescent yield and stability.[13-17] Some researches attempted to obtain perfect emission spectra by changing the substitution of PPV chain in order to improve its optical properties. For example, as early as in 1933, Greenham and his colleagues[18] synthesized a fluorescent poly(cyanoterephthalylidene) (CN-PPV) with fairly good solubility, which has lower energy gap and can enhance EL efficiency. Furthermore, some other groups reported that PPV derivatives with other specific characteristics such as poly(2-methoxy-5-(2'-ethylhexyloxy)-*p*-phenylenevinylene) (MEH-PPV) and poly(*p*-phenylenevinylene) (C-ppv) had also been synthesized.[19]

As the typical illuminant materials, the excellent electronic and optical properties will be anticipated by designing a certain kind of polymer where Alq_3 can be grafted on PPV based on the idea of molecular tailor, and some important excited states of the designed materials are studied. However, a lot of computational cost

* E-mail: zmsu@nenu.edu.cn; Tel.: 0086-0431-85099108; Fax: 0086-0431-85894009
Received February 22, 2009; revised April 29, 2009; accepted June 22, 2009.
Project supported by the National Natural Science Foundation of China (Nos. 20160025 and 20243003) and Trans-century Training Program Foundation for the Talents by the State Education Ministry of China.

must be requested to model computational details when the systems become larger and more complex. Generally speaking, the computational time t_{CPU} is proportional to certain power of the system size, *i.e.*, $t_{CPU} \propto N^x$, where N is the number of electrons, and x is an exponent, which is usually larger than 1. For instance, the computational time of *ab initio* Hartree-Fock (HF) molecular orbital calculation has an O (N^{3-4}) scaling. Therefore, in order to obtain abundant information with short computational cost, some theoretical chemists tried to develop a method that makes computational time linearly scaling to system size, *i.e.*, $t_{CPU} \propto N$. In 1996, Yang[20] employed the linear scaling semiempirical theory called "divide-and-conquer" to calculate the large molecule, and accomplished a protein systemic computation with a more than 9000 atomic number. Mukamel and Tretiak *et al.*[21-23] utilized collective electronic oscillator (CEO) to calculate molecular excited state based on the same mechanism and obtained reasonable compromise between the numerical accuracy and computational cost. However, the localized density matrix theory (LDM) had been developed by Chen group.[14-16,24-26] Its advantages lie in decreasing the computational time since the number of matrix elements is reduced in the density matrix in the equation of motion. So the LDM method is the linear-scaling quantum chemistry method by simulating molecular excited state properties, such as optical, electric and magnetic properties, even in the large molecular systems. The LDM method is based on the time-dependent Hartree-Fock (TDHF) approximation, which includes all single electron excitations and partial double, triple and the other multiple electron excitations[15] and "the nearsightedness of equilibrium systems". The UV-Vis spectra of carbon nano tubes and silicon carbide nanocrystals have already been calculated by LDM and the consistent results with those in the experiment obtained.[27-29]

Computational detail

In the present paper, density functional theory (DFT) calculations at Becke's three-parameter hybrid functional (referred as B3LYP[30,31]) with the 6-31G* basis set were used to optimize the structures and obtain frontier molecular orbitals (FMOs). Tri-(8-hydorxyquinoline)-[6-((*E*)-2-(8-hydroxyquinolin-3-yl)vinyl)-3-((*E*)-2-(8-hydroxyquinolin-6-yl)vinyl)quinolin-8-olate] (**1**), PPV (**2**), PPV-hydro [3-(4-((*E*)-2-(8-hydroxy-3-(4-styrylstyryl)-quinolin-6-yl)vinyl)styryl)-6-(4-styrylstyryl)quinolin-8-olate] (**3**) and PPV-Alq_3 (**4**) are shown in Figure 1.

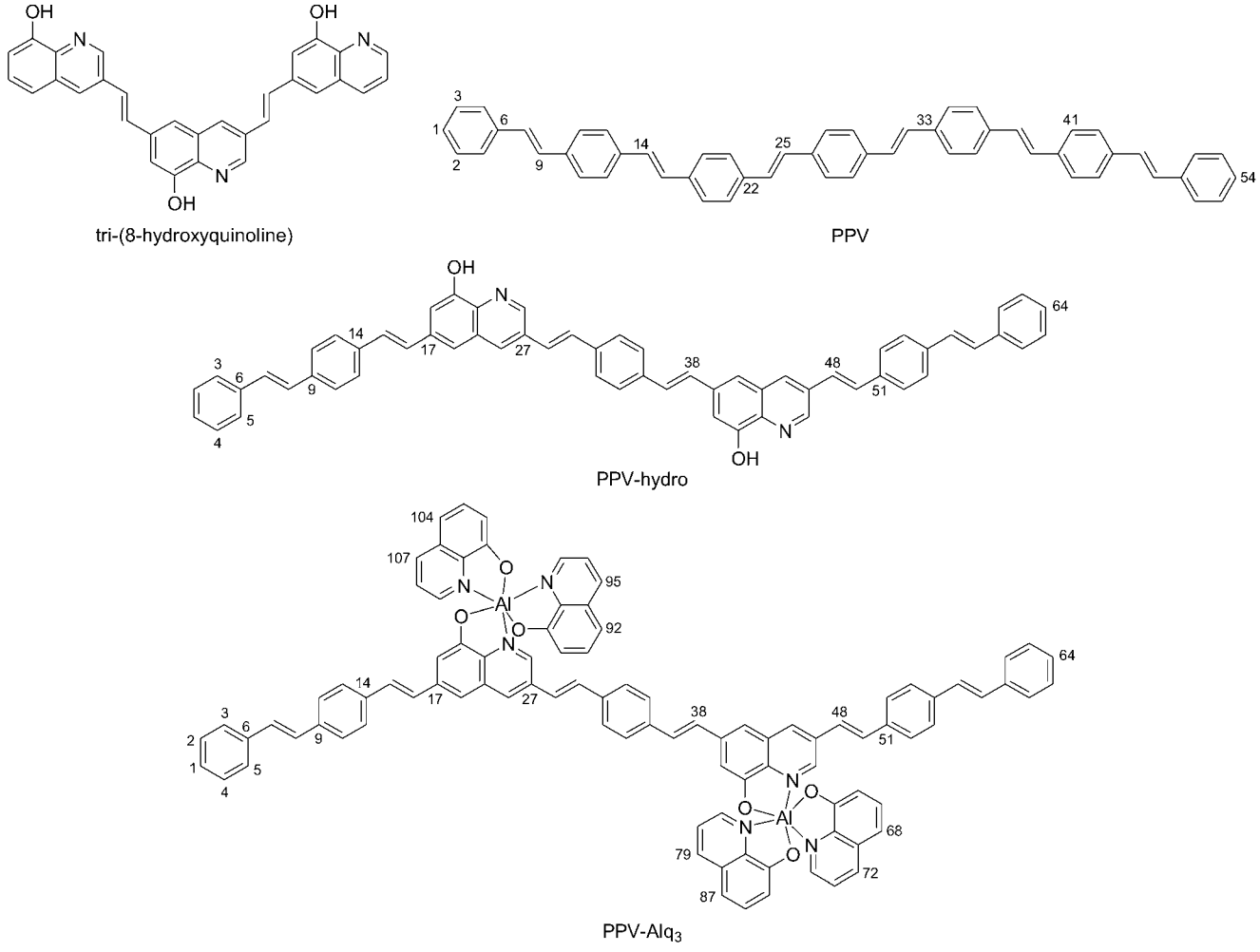

Figure 1 Molecular structures of tri-(8-hydroxyquinoline), PPV, PPV-hydro and PPV-Alq_3.

Previous calculations were performed with the Gaussian 03 program.[32] Based on the optimized stable structures, intermediate neglect of differential overlap (INDO) and LDM methods were employed to the subsequent calculations. The transition properties were obtained by INDO program and the electronic densities were received by LDM theory. Meanwhile, there are two steps in the calculation of electronic density. One is the ground state calculation and the other is the time domain exited state calculations. Reduced single electron density matrices were obtained by using LODESTAR program.[26-28]

Results and discussion

Geometry and transition

The optimizations of the species at the level of B3LYP with the 6-31G* basis set are in one plane except for PPV-Alq_3, because the addition of Alq_3 breaks the plane structure of PPV. The benzenes connected with 8-hydroxyquinolines in the main chain are distorted (the dihedral is in the range of 8°——8° for 8-hydroxyquinolines in the main chain).

The absorption spectrum of the species can be obtained by using LDM models, as shown in Figure 2. As can be seen, for PPV, its π-conjugation length is the largest so that it should have the lowest energy excitation among all the species. For tri-(8-hydroxyquinoline), it shows the highest excitation energy and lowest oscillator strength, due to its shortest π-conjugation. The transition energies of PPV and PPV-Alq_3 are just between those of tri-(8-hydroxyquinoline) and PPV. For PPV-Alq_3, it has steric hindrance coming from Alq_3, and thus is twisted to the larger extent so that it should have the higher energy excitation.

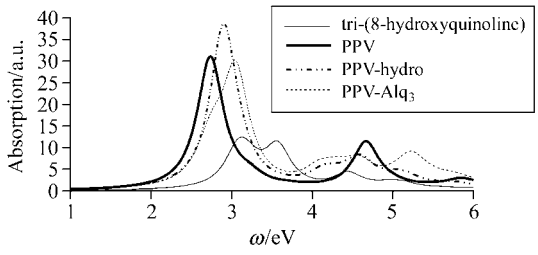

Figure 2 Absorption spectra of tri-(8-hydroxyquinoline), PPV, PPV-hydro and PPV-Alq_3.

Meanwhile, the electronic transition properties listed in Table 1 were obtained by INDO and LODESTAR program. Energy gaps show orbital energy difference between HOMO and LUMO. For the oligomer PPV, the transition of first absorption peak is mainly from HOMO to LUMO. For the PPV-hydro, the first absorption peaks come from the transition between HOMO−1 and LUMO. For the PPV-Alq_3, the first absorption peaks come from the transition between HOMO−1 and LUMO+1. However, another characteristic absorption peak of the PPV-Alq_3 comes from the HOMO−2 to LUMO+13, which is important to the subsequent discussions. Although the values of optical gap from the LDM theory are not the same as those from the INDO program, the trends of the change are consistent.

FMO and electronic densities

It is well known that the electron density distribution is important for luminescence in a molecule, those residing in the FMO are least bound to the molecule and thus are most closely related to the charge transport properties of the material. In the Figure 3, we plotted the FMO of the first dipole-allowed excited states corresponding to PPV (A), PPV-hydro (B) and PPV-Alq_3 (C), and FMO of the D is another characteristic transition at 237 nm for PPV-Alq_3. For the A, B and C, the highest occupied π orbitals and the lowest unoccupied π* orbitals mainly located on the main chain are along the stretched direction of molecule. But for the subordinated peak of infrared area of PPV-Alq_3 at 237 nm, the transition configurations are completely different, are shown from individual QH with large contribution from the two different Alq_3 moieties. D is another important excited state for PPV-Alq_3.

In order to interpret the transition properties, the contour plots (A), (B) and (C) of density matrices of the first peak are shown in Figure 4 corresponding to PPV, PPV-hydro and PPV-Alq_3, respectively. The representations of coordinates are the atom orbitals in Figure 4. The diagonal part is the electron occupation number of each orbital and the off diagonal part represents the electron-electron coherence, and the larger density matrix elements have the darker corresponding dots.

We may compare the relative coherence sizes of the excitation size for the three molecules by examining the width of the dark stripes or bandwidth in the density matrix contour plots, the width of the three molecules increases in the order PPV-Alq_3＜PPV-hydro＜PPV. It is evident that PPV-Alq_3 has the smallest size and PPV

Table 1 The properties of transition with INDO and LDM methods

	Optical gap with INDO/nm	Oscillator strength	Transition orbital	Configuration	Optical gap with LDM/nm
PPV	430.0	4.58	HOMO-LUMO	0.62	452
PPV-hydro	402.3	5.90	HOMO−1-LUMO	0.11	426
PPV-Alq_3	372.8	5.12	HOMO−1-LUMO+1	0.16	413
PPV-Alq_3	238.3	1.62	HOMO−2-LUMO+13	0.40	237

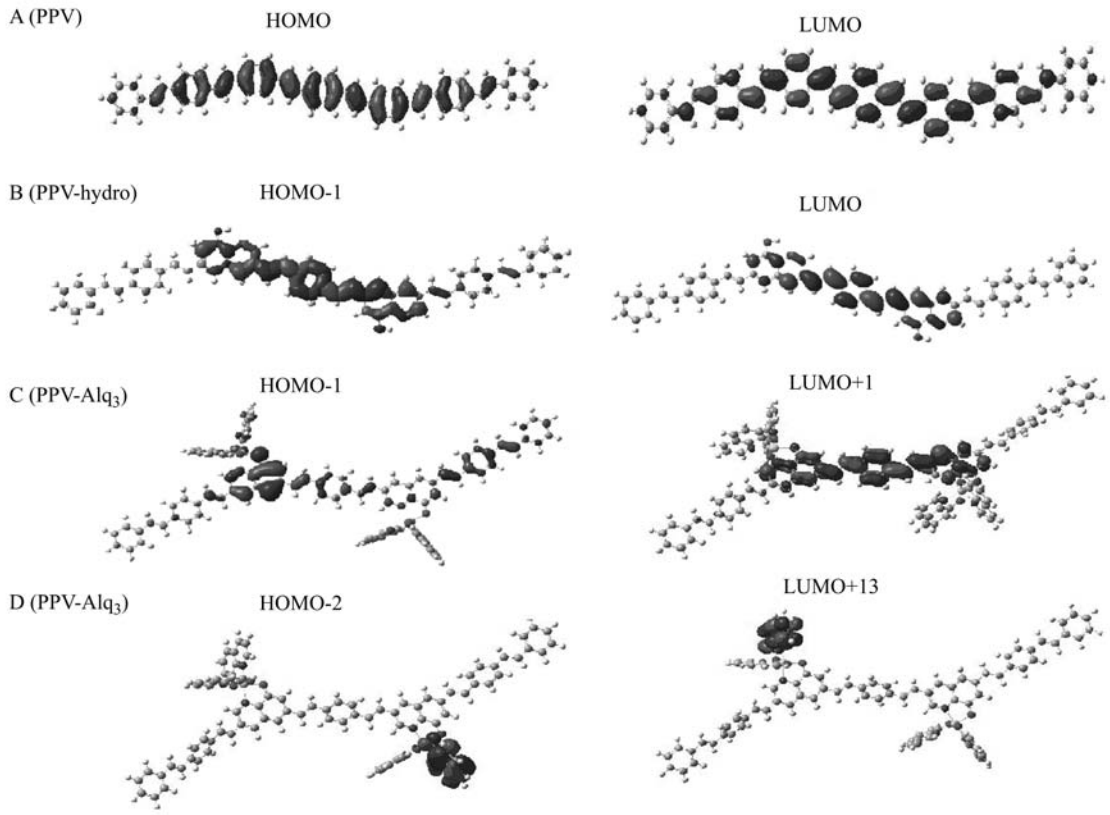

Figure 3 FMO of A, B and C plotted by first dipole-allowed excited state, FMO of D plotted important excited state of Alq_3.

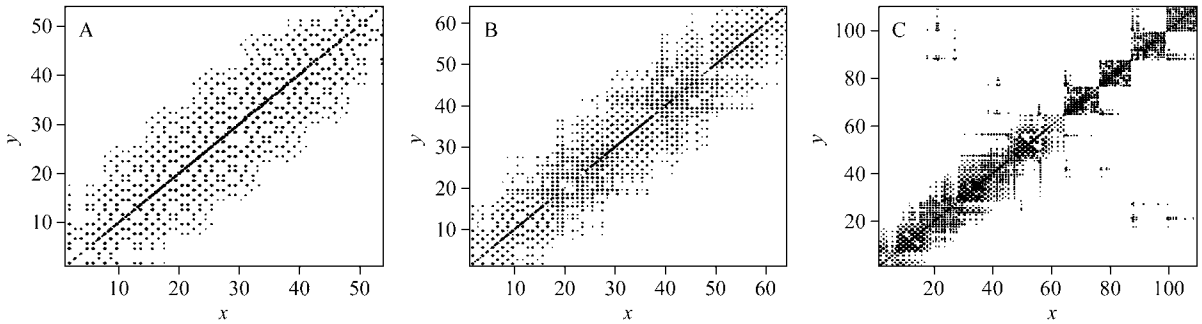

Figure 4 Contour plots of density matrices of PPV (A) $E(t)=2.74$ eV at 452 nm, PPV-hydro (B) $E(t)=2.91$ eV at 426 nm, and PPV-Alq_3 (C) $E(t)=3.00$ eV at 413 nm. *x*-*y* axes represent the indices of atom orbitals in Figure 1.

has the best conjugated character in consistent with the aforementioned arguments of the FMO. In addition, it has been shown in Figure 4(A) that uninterrupted darker plots appeared on diagonal, interpreting that there are strongly mutual effects among the atom orbitals. The (B) and (C) are weaker than the (A), especially (C). For the (B) in Figure 4, atom orbitals 1—17, 27—38 and 48—64 on the benzene also have strongly mutual effects.

It is consistent with the properties from the picture (B) in Figure 3, which proves that LDM could excellently explain mutual effects between the atom orbitals. As can be seen from the (C) in Figure 4, orbitals from coordinate 10 to 50 are responsible for the excited state, which comes from the contribution of benzene and QH in the main chain. But, the weak effects are observed where the coordinate from orbital 64 to 110 of QH in the side chains is negligible.

Comparison for different excitation of PPV-Alq_3 by LDM theory

In order to reveal the properties of different excited states, PPV-Alq_3 was divided into three segments, which are shown in Figure 5(A). Segment 1 along the extended direction of the molecule means the main chain, corresponding to the first 64 orbitals. Segment 2 and segment 3 connected to the main chain by Al were divided into two parts, which are located on the two sides of the main chain. They are corresponding to orbitals 65—87 and 88—110, respectively. So, Figure 5 shows the excited state density matrixes corresponding

to the two different peaks of PPV-Alq_3, $E(t)=3.00$ eV (B) and $E(t)=5.23$ eV (C) obtained by the LDM theory. The intensities of matrix elements are very sensitive to the distance between the orbitals. Figure 5(B) exhibits the typical feature of excited state density matrix at $E(t)=3.00$ eV as discussed in previous section. As can be seen from the Figure 5(B), mutual effects between orbitals happened in benzenes of the main chain and are irrespective to QH of segments 2 and 3. But for the excitation in $\omega=5.23$ eV, the matrix elements of Figure 5(C) between segments 2 and 3 show the dark area from 76 to 87 because of the mutual effects of two QH moieties. It induced a change of $\partial\rho$ in the reduced density matrix and in turn the electronic transition formed. Surprisingly, Figure 5(C) shows almost identical results as the FMO. Thus, it is important to calculate the density matrix to investigate the excited configuration.

Conclusion

Electronic properties of polymerized Alq_3 and 8-hydroxyquinoline grafted on PPV units were discussed by the LDM method. (I) The results from the FMO, the absorption peak and density matrices are generally coherent. The strongest absorption peaks show red shift from the 8-hydroxyquinoline, PPV-Alq_3, PPV-hydro to PPV. (II) For PPV-Alq_3, absorption peak is at 413 nm near the purple light. Two 8-hydroxyquinolines have very slight contribution to electronic transition. Another absorption peak is at 237 nm. The characteristic peak of PPV-Alq_3 is completely different from the first one. It comes from contribution of 8-hydroxyquinolines in the two different side chains. (III) LDM theory is more effective to obtain absorption spectra and electronic properties than other theories, which usually need a large computational cost.

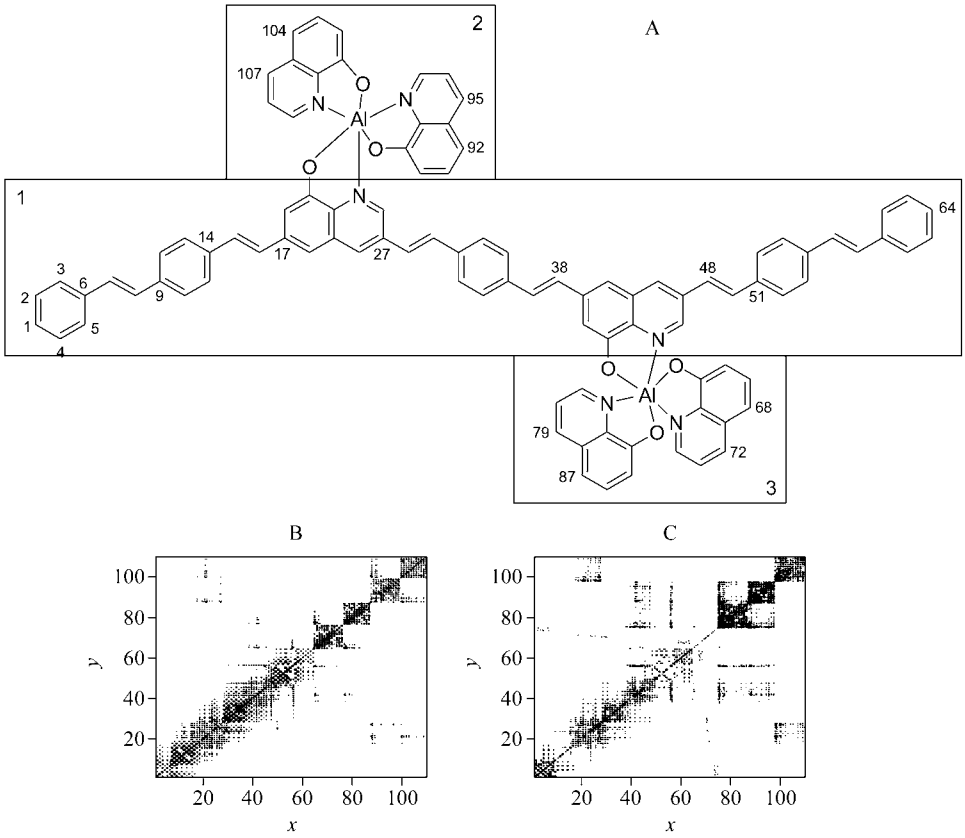

Figure 5 Contour plots of density matrices for the PPV-Alq_3 respectively in $E(t)=3.00$ eV and $E(t)=5.225$ eV. *x*-*y* axes represent the indices of atom orbitals of Alq_3.

References

1 Tang, C. W.; Vanslyke, S. A. *Appl. Phys. Lett*. **1987**, *51*, 913.

2 Ozasa, K.; Nemoto, S.; Isoshirna, T.; Ito, E.; Maeda, M.; Hara, M. *Surf. Interface Anal*. **2008**, *40*, 810.

3 Kim, E. S.; Kim, K.; Jin, J. I.; Choi, J. H. *Synth. Met*. **2001**, *121*, 1677.

4 Chen, W.; Peng, Q.; Li, Y. *Adv. Mater*. **2008**, *20*, 2747.

5 Hua, R. N.; Niu, J. H.; Yu, T. Z.; Hong, Z. R.; Li, W. L.; Fan, S. D. *Chin. J. Chem*. **2008**, *26*, 775.

6 Mario, A.; Francesco, L. *J. Phys. Chem. A* **2003**, *107*, 2560.

7 Kan, Y. H.; Zhu, Y. L.; Hou, L. H.; Su, Z. M. *Acta Chim. Sinica* **2005**, *63*, 1623 (in Chinese).

8 Kwiatkouski, J. J.; Nelso, J.; Li, H.; Bredas, J. L.; Wenzel, W.; Lennartz, C. *Phys. Chem. Chem. Phys*. **2008**, *10*, 1852.

9 Irfan, A.; Cui, R. H.; Zhang, J. P. *J. Mol. Struct*. **2008**, *850*, 79.
10 Gao, H. Z.; Su, Z. M.; Qin, C. S.; Mo, R. G.; Kan, Y. H. *Int. J. Quantum Chem*. **2004**, *97*, 992.
11 Liao, Y.; Chen, Y. G.; Su, Z. M.; Kan, Y. H.; Duan, H. X.; Zhu, D. X. *Synth. Met*. **2003**, *137*, 1093.
12 Burroughes, J. H.; Bradley, D. C.; Brown, A. R.; Marks, R. N.; Marks, K.; Mackay, K.; Friend, R. H.; Burn, P. L.; Holmes, A. B. *Nature* **1990**, *347*, 539.
13 Cornil, J.; Santos, D. A.; Crispin, X.; Silbey, R.; Bredas, J. L. *J. Am. Chem. Soc*. **1998**, *120*, 1289.
14 Yokojima, S.; Zhou, D. H.; Chen, G. H. *Chem. Phys. Lett*. **2001**, *333*, 397.
15 Ng, M. F.; Yokojima, S.; Zhou, D. H.; Chen, G. H. *Chem. Phys. Lett*. **2000**, *327*, 374.
16 Ng, M. F.; Sun, S. L.; Zhang, R. Q. *J. Appl. Phys*. **2005**, *97*, 103513.
17 Kraft, A.; Grimsdale, A. C.; holmes, A. B. *Angew. Chem., Int. Ed*. **1998**, *37*, 402.
18 Greenham, N. C.; Moratt, S. C.; Bradley, D. C.; Friend, R. H.; Holmes, A. B. *Nature* **1993**, *365*, 628.
19 Wang, S.; Liu, Y. Q.; Liu, H. W.; Yu, G.; Xu, Y.; Zhan, X. W.; Xi, F.; Zhu, D. B. *J. Phys. Chem. B* **2002**, *106*, 10618.
20 Lee, T. S.; York, D. M.; Yang, W. T. *J. Chem. Phys*. **1996**, *105*, 2744.
21 Mukamel, S.; Tretiak, S.; Wagersreiter, T.; Chernyak, V. *Science* **1997**, *277*, 781.
22 Tretiak, S.; Mukamel, S. *Chem. Rev*. **2002**, *102*, 3171.
23 Franco, I.; Tretiak, S. *J. Am. Chem. Soc*. **2004**, *126*, 12130.
24 Yam, C. Y.; Yokojima, S.; Chen, G. H. *J. Chem. Phys*. **2003**, *119*, 8794.
25 Wang, F.; Yam, C. Y.; Chen, G. H. *J. Chem. Phys*. **2007**, *126*, 244102.
26 Yokojima, S.; Chen, G. H. *Phys. Rev. B* **1999**, *59*, 7259.
27 Liang, W. Z.; Yokojima, S.; Zhou, D. H.; Chen, G. H. *J. Phys. Chem. A* **2000**, *104*, 2445.
28 Liang, W. Z.; Yokojima, S.; Ng, M. F.; Chen, G. H.; He, G. *J. Am. Chem. Soc*. **2001**, *123*, 9830.
29 Shi, S. L.; Xu, S. J.; Wang, X. J.; Chen, G. H. *Thin Solid Films* **2006**, *495*, 404.
30 Lee, C.; Yang, W.; Parr, R. G. *Phys. Rev. B* **1998**, *37*, 785.
31 Becke, A. D. *J. Phys. Chem*. **1993**, *98*, 5648.
32 Frisch, M. J.; Trucks, G. W.; Schlegel, H. B.; Scuseria, G. E.; Robb, M. A.; Cheeseman, J. R.; Montgomery, J. A. Jr.; Vreven, T.; Kudin, K. N.; Burant, J. C.; Millam, J. M.; Iyengar, S. S.; Tomasi, J.; Barone, V.; Mennucci, B.; Cossi, M.; Scalmani, G.; Rega, N.; Petersson, G. A.; Nakajima, T.; Honda, Y.; Kitao, O.; Nakai, H.; Klene, M.; Li, X.; Knox, J. E.; Hratchian, H. P.; Cross, J. B.; Adamo, C.; Jaramillo, J.; Gomperts, R.; Stratmann, R. E.; Yazyev, O.; Austin, A. J.; Cammi, R.; Pomelli, C.; Ochterski, J. W.; Ayala, P. Y.; Morokuma, K.; Voth, J. A.; Salvador, P.; Dannenberg, J. J.; Zakrzewski, V. G.; Dapprich, S.; Daniels, A. D.; Strain, M. C.; Farkas, O.; Malick, D. K.; Rabuck, A. D.; Raghavachari, K.; Foresman, J. B.; Ortiz, J. V.; Cui, Q.; Baboul, A. G.; Clifford, S.; Cioslowski, J.; Stefanov, B. B.; Liu, G.; Liashenko, A.; Piskorz, P.; Komaromi, I.; Martin, R. L.; Fox, D. J.; Keith, T.; Al-Laham, M. A.; Peng, C. Y.; Nanayakkara, A.; Challacombe, M.; Gill, P. M. W.; Johnson, B.; Chen, W.; Wong, M. W.; Gonzalez, C.; Pople, J. A. *Gaussian 03*, Revision C. 02, Gaussian, Inc., Wallingford CT, **2004**.

(E0902224 Cheng, B.; Zheng, G.)